

## RAMAN SCATTERING UTILIZATION FOR DISTRIBUTED TEMPERATURE MEASUREMENT IN OPTICAL FIBRES

Robert CYBULSKI<sup>1</sup>, Krzysztof PERLICKI<sup>1</sup>, Mirosław SIERGIEJCZYK<sup>2</sup>

<sup>1</sup>Warsaw University of Technology, Faculty of Electronics and Information Technology,

<sup>2</sup>Warsaw University of Technology, Faculty of Transport

e-mail: [R.Cybulski@tele.pw.edu.pl](mailto:R.Cybulski@tele.pw.edu.pl)

### Summary

Concept of fibre spontaneous Raman scattering utilizing for distributed temperature sensing is presented. Chosen approach uses both backscattered Stokes as reference and anti-Stokes as detection signals. The analysis is carried out towards Stokes and anti-Stokes bands temperature dependence. In order to achieve best measurement accuracy influence of maximum modulation frequency on spatial resolution is verified. Analysed technique allows to calculate temperature along the fibre with 5 m space precision and 1°C temperature precision. Simulations involve 200 m standard single mode fibre in temperatures in range  $< -5^{\circ}\text{C}, 60^{\circ}\text{C} >$  with 2x1100 m reference fibre maintained in 22°C.

Keywords: scattering, Raman, temperature, measurement

### WYKORZYSTANIE ROZPRASZANIA DO POMIARU TEMPERATURY WE WŁÓKNIE ŚWIATŁOWODOWYM

Koncepcja wykorzystania rozpraszania Ramana we włóknie światłowodowym do rozproszonego pomiaru temperatury została przedstawiona. W wykorzystanym podejściu użyto zarówno światła rozpraszania Stokes'a i anti-Stokes'a odpowiednio jako sygnałów odniesienia i czujnikowego. Analiza opiera się na fakcie zależności rozpraszania w pasmach Stokes'a i anti-Stokes'a od temperatury. W celu optymalizacji jakości pomiaru oceniono wpływ maksymalnej częstotliwości modulacji lasera na przestrzenną rozdzielczość pomiaru. W analizowanym przypadku oraz przy przyjętych wartościach parametrów możliwa jest realizacji pomiaru z dokładnością przestrzenną na poziomie 5 m i temperaturową 1 °C. W symulacjach badany jest odcinek 200 m światłowodu czujnikowego G.652 w temperaturach z zakresu  $< -5^{\circ}\text{C}, 60^{\circ}\text{C} >$  oraz dwóch odcinków światłowodu odniesienia od długości 1100 m w temperaturze pokojowej 22°C.

Słowa kluczowe: rozpraszanie światła, Raman, temperatura, pomiar

## 1. INTRODUCTION

Properties of optical fibres give several more their applications than just high speed data transmission. One of these applications is temperature sensing by means of backscattered light analysis where another. Of course backscattered light can be used otherwise like for example for fibre birefringence distribution evaluation [1, 2]. It is known that change in external conditions (temperature, pressure etc.) has its influence on the properties of light propagation in a fibre and so it is in the case of light that scatters on the SiO<sub>2</sub> molecules reflects and travels backward. There are several different ways to use this process in order to obtain information about changes of environmental conditions. This division is based on choosing different backscattered detection signal, which is susceptible on changes of temperature and reference signal which is usually much stronger than the latter

and therefore can be regarded as insensitive for these kind of changes. Most efficient solutions employ Raman scattering Stokes and anti-Stokes waves, respectively as reference and detection signals [3-6] or Raman (anti-Stokes) and Rayleigh backscattered signals [3]. An interesting concept is presented in [7] where Brillouin together with Rayleigh scattering are used respectively as detection signal (pulse scattered by interaction with acoustic wave) and reference signal (Rayleigh scattered pulse base). This approach however demands highly sensitive photon counting in receiver because of low level Brillouin scattered signal. Brillouin scattering is also used for temperature changes detection in [8] where slow light generation is obtained by acoustic wave influence on refractive index. Changes of the temperature cause difference in the Brillouin frequency shift and therefore the velocity of propagating light changes. This fact is used to

establish the relative delay between two pulses propagating in opposite directions. Different approach is presented in [9] and it is based on frequency spectrum analysis of the signal reflected backwards on the number of fibre Bragg gratings with different grating constants, created on testing fibre. Changes of temperature around fibre fragment where Bragg grating is performed shall cause modification of its grating constant and therefore spectrum of reflected signal also changes. By monitoring the spectrum of reflected signal in receiver one can establish the location of the disturbance. Significant disadvantages of this solution are limited spatial resolution imposed by limited capability of performing gratings on specific length of fibre and the level of difficulty in preparing such detection fibre. From all these methods authors choose usage the Raman Stokes and anti-Stokes backscattered signals which gives the spatial resolution of 5 m and temperature resolution of 1°C. One of the applications of distributed temperature sensor could be performance monitoring of power supply units [10, 11, 12].

## 2. MATHEMATICAL MODEL

Raman scattering occurs when incident light interacts with material structure irregularities which comes in two scenarios:

- incident photon loses part of its energy for quant of structure vibration energy – creates optical phonon. Rest of the photon energy is emitted as new photon (Stokes photon) of lower energy (lower frequency) than incident one
- creation of anti-Stokes photon from incident photon and optical phonon. Photon absorbs phonon energy therefore anti-Stokes photon has higher frequency and energy. It is important to notice that anti-Stokes photon creation is more complicated process than in case Stokes creation, because it demands phase and energy match between phonon and incident photon. That is why the probability of anti-Stokes photon generation is lower than Stokes photon generation and so the anti-Stokes wave is weaker than Stokes wave [3-6].

Knowing that it is clear that anti-Stokes wave is more susceptible on temperature changes and therefore in the analyzed model anti-Stokes wave is considered as detection signal and Stokes wave is the reference signal. The ratio of powers of these two waves is shown in described in [3] and [5] mathematical model. Power of cosine modulated wave propagating in the +z direction of the fibre is described by equation:

$$P(z, \omega, t) = P_0 e^{-\alpha_P z} (1 + m \cos(\omega(t - \beta_P z))) \quad (1)$$

where  $P_0$  is initial power of incident light,  $\alpha_P$  – attenuation coefficient at the pump wavelength,  $m$  is the modulation coefficient,  $\omega$  – radial frequency,  $\beta_P$  – propagation constant value at pump wavelength. There are two components in the (1) equation but only second carries information dependent on the modulation frequency and will be taken for further analysis. The amount of light scattered from dz fragment of fibre in equations (2) and (3) is proportional to the number of phonons in specific temperature. The coefficient representing this fact and also depend on the material itself is the  $\chi_S$  for Stokes and  $\chi_{AS}$  for anti-Stokes waves [3, 5]:

$$dP_S(z, \omega, t) = \chi_S m P_0 e^{-(\alpha_P + \alpha_S)z} \cos(\omega(t - (\beta_P + \beta_S)z)) dz, \quad (2)$$

$$dP_{AS}(z, \omega, t) = \chi_{AS} m P_0 e^{-(\alpha_P + \alpha_{AS})z} \cos(\omega(t - (\beta_P + \beta_{AS})z)) dz, \quad (3)$$

where  $\alpha_S$  and  $\alpha_{AS}$  are attenuation coefficients respectively for Stokes and anti-Stokes waves,  $\beta_S$  and  $\beta_{AS}$  are propagation constants for Stokes and anti-Stokes. Total backscattered light from dz parts of fibre of length L detected at the receiver is described as [3, 5]:

$$P_R(0, \omega, t) = \int_0^L \chi_R m P_0 e^{-\alpha_T z} \cos(\omega(t - \beta_T z)) dz. \quad (4)$$

Where subscript R stands for Stokes or anti-Stokes and  $\beta_T = \beta_R + \beta_P$  and  $\alpha_T = \alpha_R + \alpha_P$ . In the matter of computer simulations it is useful to divide fibre in M parts each with different  $\chi$  value. Under such condition equation (4) is converted [3]:

$$P_R(0, \omega, t) = m P_0 \sum_{k=1}^M \chi_k e^{\alpha_T \sum_{j=1}^k D_j - D_{j-1}} \int_{D_{k-1}}^{D_k} e^{-\alpha_T(z - D_k)} \cos(\omega(t - \beta_T z)) dz. \quad (5)$$

Equation (4) can be regarded as Fourier transform as  $\chi_R(T)$  therefore the main principle of temperature measurement is that having frequency response of the fibre measured in the receiver one can calculate the inverse Fourier. In that way it is possible to evaluate  $\chi_R$  value for every measurement point [3, 5]:

$$\chi_R(z) = IFFT(P_R)/(m P_0 e^{-\alpha_T z}), \quad (6)$$

Distributed temperature profile can be calculated as [3, 5]:

$$T(z) = 1 / \left( \frac{1}{T_0} + \frac{k_B}{\hbar \omega_P} \ln \left( \frac{R_0}{R_1} \right) \right), \quad (7)$$

where  $k_B$  – the Boltzmann constant,  $\hbar$  – normalized Planck constant,  $\omega_P$  – pump wavelength,  $R_0$  is the

power level ratio coefficient between Stokes and anti-Stokes waves [3, 5]:

$$R_0 = \frac{n_{AS}\lambda_S^4}{n_S\lambda_{AS}^4} e^{\frac{h\omega_P}{k_B T_0}}, \quad (8)$$

where  $n_{AS}$  and  $n_S$  – refractive indexes for anti-Stokes and Stokes wavelength,  $\lambda_S^4$  and  $\lambda_{AS}^4$  – Stokes and anti-Stokes wavelength.  $R_0$  value is approximately equal  $e^{\frac{h\omega_P}{k_B T_0}}$  which means that in room temperature Stokes wave is about 10 times stronger than anti-Stokes wave. This value is dropping with temperature rising therefore the resolution of whole process is getting worse with growth of the temperature and is better for lower temperatures. The  $R_1$  value is described as [2,4]:

$$R_1 = \frac{\chi_{AS}(z)}{\chi_S(z)} e^{-(\alpha_S - \alpha_{AS})z} \quad (9)$$

The spatial resolution value is connected with the maximum modulation frequency value  $f_{max}$  by equation [3]:

$$\Delta z = \frac{c}{2n_g f_{max}} \quad (10)$$

where  $n_g$ - refractive group index. It can be calculated that having 20 MHz source generator it is possible achieve spatial resolution of value approximately 5 m.

For noise consideration it is assumed that main contribution to the noise power is imposed by shot noise and thermal noise. Equations 10 and 11 describe total powers of shot and thermal noise respectively, where equation 12 describes the SNR figure [13].

$$\sigma_S^2 = 2qM^2 F_A (RP_{in} + I_d) \Delta f, \quad (11)$$

$$\sigma_T^2 = 4 \left( \frac{k_B T}{R_L} \right) F_n \Delta f, \quad (12)$$

$$SNR = \frac{(MRP_{in})^2}{\sigma_S^2 + \sigma_T^2}, \quad (13)$$

Values of required parameters are based on the data sheet of Thorcat PDA10CS. The mean value of SNR versus modulation frequency is approximately 23 dB.

### 3. SIMULATION RESULTS

Testing scheme investigated in simulation is presented in figure 1. It consists of 200m testing G.652 fibre in temperatures: -5°C, 16°C, 27°C, 36°C, 51°C and 2x 1100 m of reference g.652 fibre. As a result of simulation frequency response of the fibre, Stokes and anti-Stokes signals phases and distributed temperature profile will be presented. However in case of Stokes signal according to the

theory it is assumed that its phase will not change with temperature.

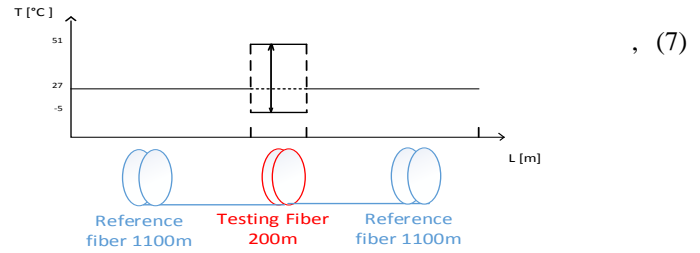


Fig.1. Simulation scheme

#### 3.1. Case 1 – sensing fibre at 60°C

Figures 2, 3, 4 and 5 show frequency response of the fibre anti-Stokes signal phase, Stokes signal phase and temperature distribution respectively for scenario of sensing fibre at 60°C.

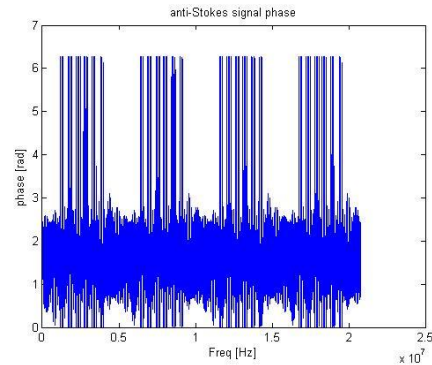


Fig. 2. Anti-Stokes signal phase for 60°C

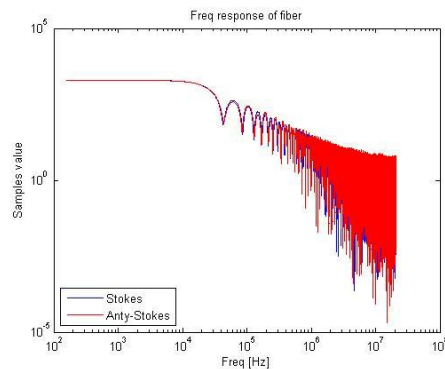


Fig. 3. Frequency response of the fibre for 60°C

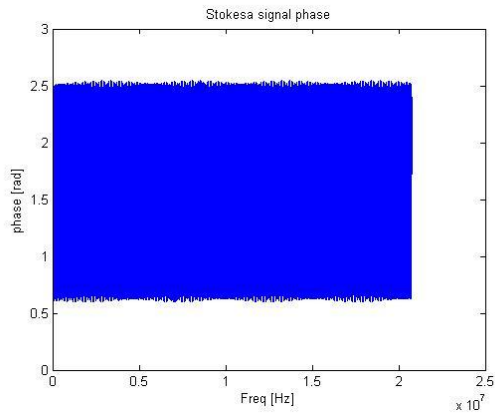


Fig. 4. Stokes signal phase for 60°C

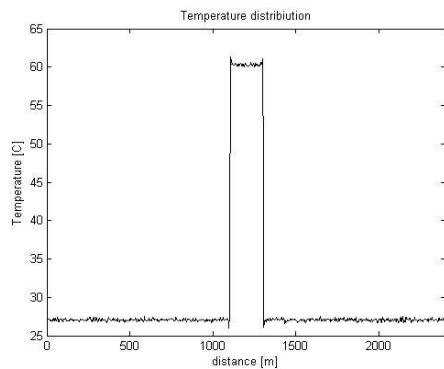


Fig. 5. Temperature profile for 60°C

### 3.2. Case 2 – sensing fibre at 35°C

Figures 6, 7, 8 and 9 show frequency response of the fibre anti-Stokes signal phase, Stokes signal phase and temperature distribution respectively for scenario of sensing fibre in 35°C.

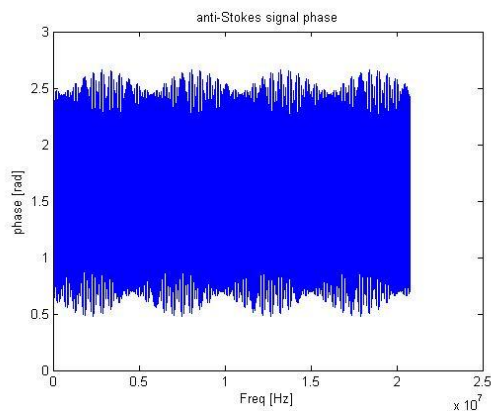


Fig. 6. Anti-Stokes signal phase for 35°C

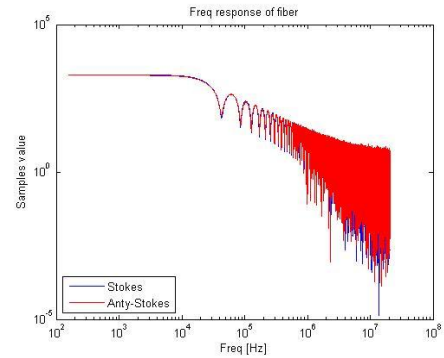


Fig. 7. Frequency response for 35°C

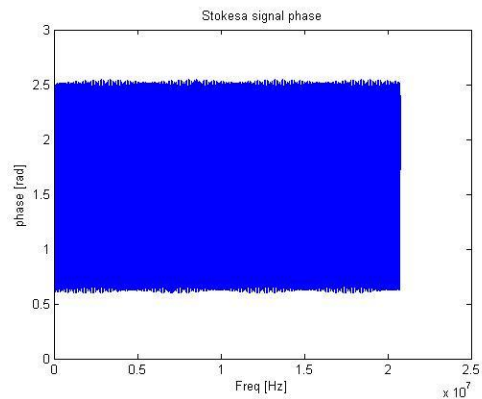


Fig. 8. Stokes signal phase for 35°C

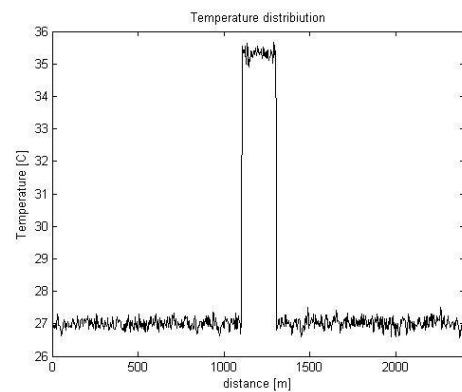


Fig. 9. Temperature profile for 35°C

### 3.3. Case 3 – sensing fibre at 27°C

Figures 10, 11, 12 and 13 show frequency response of the fibre anti-Stokes signal phase, Stokes signal phase and temperature distribution respectively for scenario of sensing fibre in 27°C.

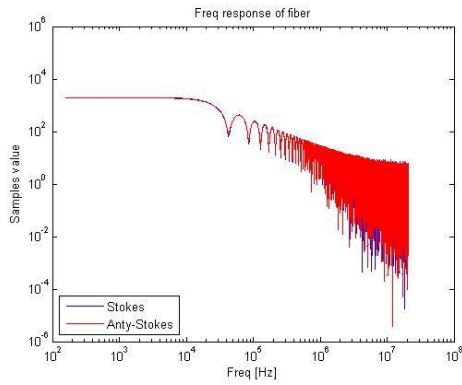


Fig. 10. Frequency response for 27°C

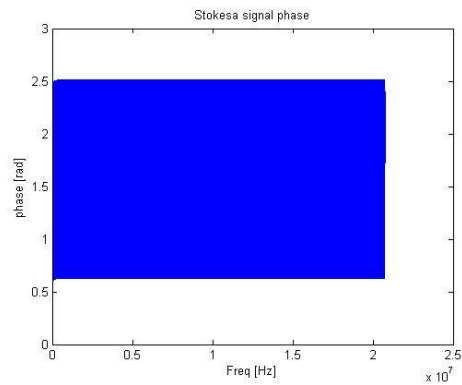


Fig. 11. Anti-Stokes signal phase for 27°C

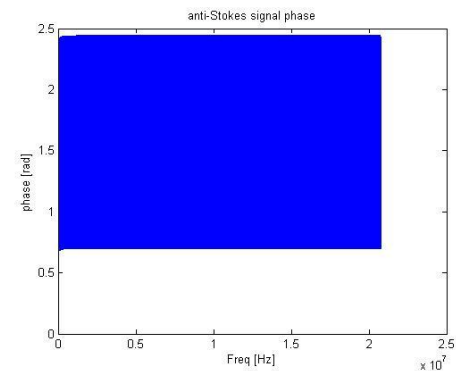


Fig. 12. Stokes signal phase for 27°C

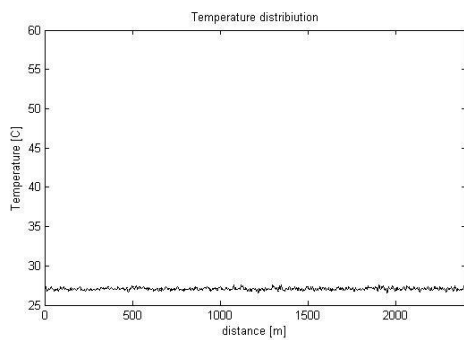


Fig. 13. Temperature profile for 27°C

### 3.4. Case 4 – sensing fibre at 16°C

Figures 14 and 15 show anti-Stokes signal phase and temperature distribution respectively for scenario of sensing fibre in 16°C.

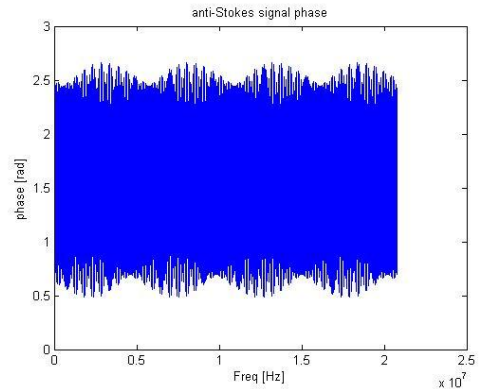


Fig. 14. Anti-Stokes signal phase for 16°C

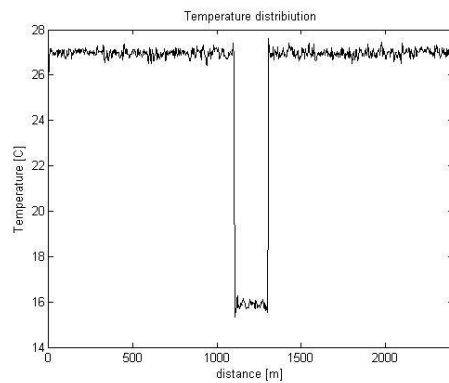


Fig. 15. Temperature profile for 16°C

### 3.5. Case 5 – sensing fibre at -5°C

Figures 16 and 17 show anti-Stokes signal phase and temperature distribution respectively for scenario of sensing fibre in -5°C.

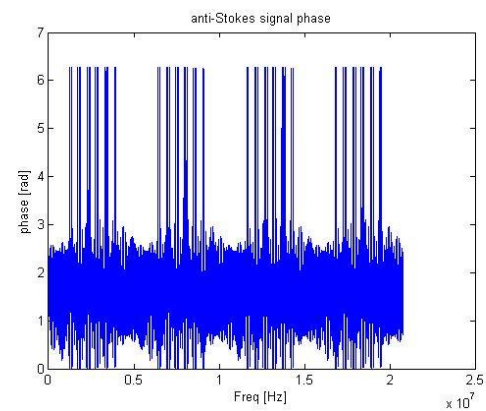


Fig. 16. Anti-Stokes signal phase for -5°C

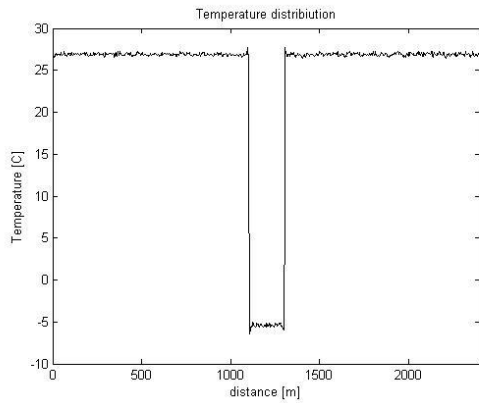


Fig. 17. Temperature profile for  $-5^{\circ}\text{C}$

Comparison between figures 2-16 shows that phase of the Stokes signal does not change with temperature therefore it can be used as reference signal. Moreover it can be seen that higher temperature affects the maximum value of the phase of anti-Stokes signal. For higher temperatures ( $60^{\circ}\text{C}$ ) maximum value of anti-Stokes signal phase grows faster than in case of lower temperatures ( $+36^{\circ}\text{C}$ ). In all these cases it is clear that frequency response of the combined fibres decays for frequency values close to maximum, which comes from solving equation (5). This frequency region is therefore responsible for lowering of mean SNR value. In further analysis graphics of frequency response and Stokes signal phases will be skipped. Figures 6 and 14 show that similar changes of temperatures below ( $16^{\circ}\text{C}$ ) and above ( $36^{\circ}\text{C}$ ) of point of balance ( $+27^{\circ}\text{C}, +27^{\circ}\text{C}, +27^{\circ}\text{C}$ ) causes similar phase change of anti-Stokes signal. The same situation is observable with temperatures  $-5^{\circ}\text{C}$  and  $60^{\circ}\text{C}$  shown at figures 2 and 15 respectively. Result of investigation of noise impact on temperature measurement is presented in figure 17. It shows temperature profile in case - sensing fibre at  $+27^{\circ}\text{C}$  but in closer zoom. This allows to notice that in presence of noise peak to peak changes of temperature values are approximately  $1^{\circ}\text{C}$  which implies the same value of temperature resolution.

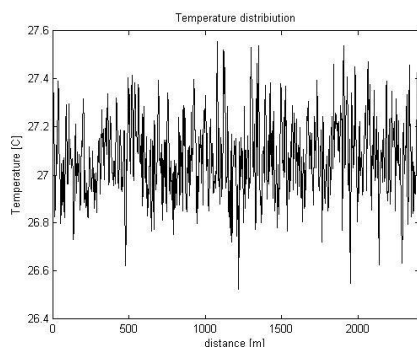


Fig. 18. Temperature variations due to the shot and thermal noise

Next impact of spatial resolution of measurement on its reliability is investigated. Figure 19 presents new configuration with spatial resolution still at value of 5 m (maximum modulation frequency equal to 20MHz). Two hot spots ( $32^{\circ}\text{C}$ ) of longitude of values of 0.5 m separated by 1 m of fibre in temperature  $27^{\circ}\text{C}$ . Figures 20 - 23 present results of such configuration simulation.

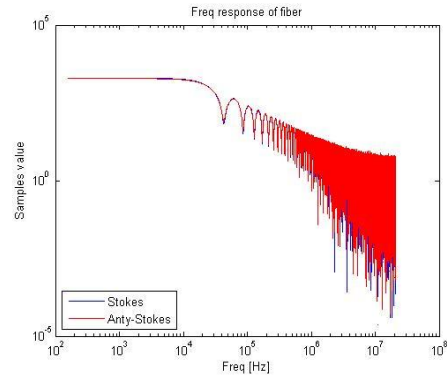


Fig. 19. Spatial resolution testing configuration

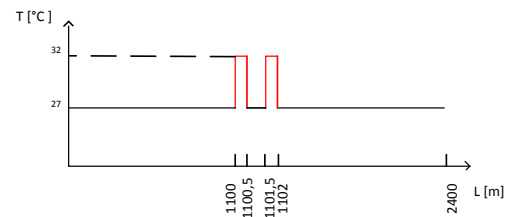


Fig. 20. Frequency response of the fibre for resolution testing configuration

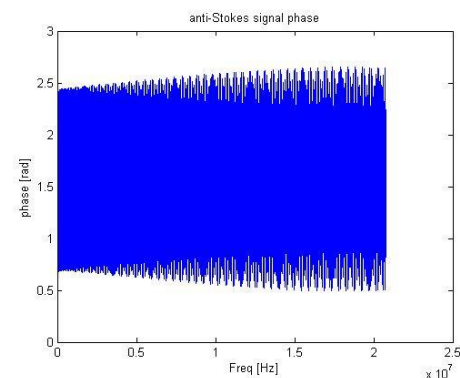


Fig. 21. Anti-Stokes signal phase for resolution testing configuration

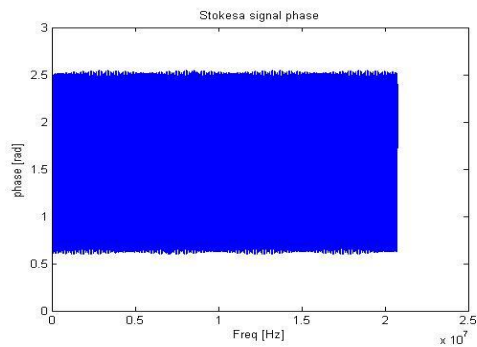


Fig. 22. Stokes signal phase for resolution testing configuration

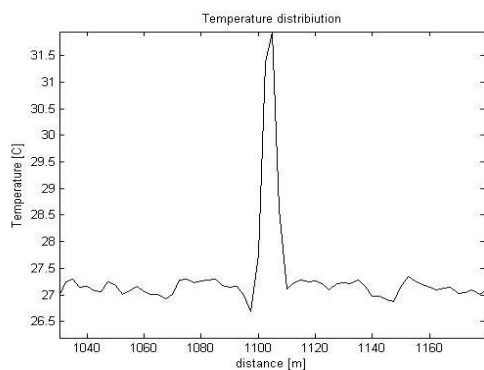


Fig. 23. Temperature profile for resolution testing configuration

Analysis of results given by figures 19 - 22 shows that anti-Stokes phase is changing in different way that in case of single hot spot. This means that anti-Stokes signal phase change is unique for each configuration which proves usability of anti-Stokes signal monitoring for distributed temperature profile evaluation at different events distribution along the fibre. Temperature profile shows that with maximum modulation frequency of 20 MHz is not correct to properly distinguish different hot spots closer to each other that calculated spatial resolution of 5 m.

#### 4. CONCLUSIONS

Presented simulation results show that stimulated Raman scattering may be used for distributed temperature sensing with accuracy of 1°C. Mean SNR value is imposed mainly by decay of the frequency response in the higher modulation frequency values. Temperature resolution is imposed by temperature stability of Stokes scattered signal in comparison to the anti-Stokes signal and as it can be seen Stokes signal is insensitive to temperature changes. Observation of the changes of anti-Stokes signal with temperatures show that below and above temperature +27°C changes of temperature results in periodical growth of maximum phase value. This facts allow to notice that observation of anti-Stokes signal phase is may

give information about temperature changes of the testing fibre with 5 m spatial precision.

#### LITERATURE

- [1] Perlicki K. Evaluation of the spatial distribution of birefringence in an optical-fiber link, *Microwave and Optical Technology Letters*, vol. 42, nr 2, pp. 147-149, 2004
- [2] Perlicki K. *Statistical PMD and PDL effects emulator based on polarization maintaining optical fiber segments*. *Optical and Quantum Electronics*, vol. 41, no. 1, pp. 1-10, 2009
- [3] Karamehmedovic E. *Incoherent optical frequency domain reflectometry for distributed thermal sensing*. Technical University of Denmark, Department of Electromagnetic System, 2006
- [4] Jingcui C., Shuguang L., Xinbo H.: *Study on Optical Fiber Temperature-Sensing Technique for Vacuum Circuit Breaker Contactor Based on Raman Scattering Theory*. *Electrical and Control Engineering (ICECE)*, 2010 International Conference on , vol., no., pp.4305-4308, 25-27 June 2010
- [5] Farahani M., Gogolla T. *Spontaneous Raman scattering in optical fibers with modulated probe light for distributed temperature Raman remote sensing*. *Journal of Lightwave Technology*, vol.17, no.8, pp.1379,1391, Aug 1999
- [6] Guo J. , Xia T., Zhang R., Li X. *A novel multimode fiber for distributed temperature sensing based on anti-stokes Raman scattering*. *Photonics Global Conference (PGC)*, 2012 , vol., no., pp.1-3, 13-16 Dec. 2012
- [7] Cui Q., Pamukcu S. , Lin A., Xiao W., Herr D., Toulouse J., Pervizpour M. *Distributed Temperature Sensing System Based on Rayleigh Scattering BOTDA*. *Sensors Journal, IEEE*, vol.11, no.2, pp.399,403, Feb. 2011
- [8] Wang L., Zhou B., Shu C., He S. *Distributed Temperature Sensing Using Stimulated-Brillouin-Scattering-Based Slow Light*. *IEEE Photonics Journal*, vol. 5, no. 6, 2013
- [9] QIAN Xiangzhong, WANG Xuelei: *FBG Based Sensing System for Temperature Monitoring of the High Voltage Apparatus*. *Journal of Proceedings of the CSU-EPSA*, vol. 19, no. 5, pp. 49-51, 2007
- [10] Rosiński A., Dąbrowski T. *Modelling reliability of uninterruptible power supply units*. *Eksploatacja i Niezawodność – Maintenance and Reliability*, vol.15, no. 4, 2013, pp. 409-413
- [11] Rosiński A. *Rationalisation of the maintenance process of transport telematics system comprising two types of periodic inspections*. In „Proceedings of the Twenty-Third International Conference on Systems Engineering”, editors: Henry Selvaraj, Dawid Zydek, Grzegorz Chmaj, given as the monographic publishing series – „Advances in intelligent systems and computing”, Vol. 1089, the publisher: Springer, 2015, pp. 663-668

- [12] Siergiejczyk M., Rosiński A. *Analysis of power supply maintenance in transport telematics system*. Solid State Phenomena, vol. 210 (2014), pp. 14-19
- [13] Agrawal G. P. *Fiber-Optic Communications Systems Third Edition*. John Wiley&Sons, 2002



**Robert CYBULSKI** received his B.Sc. degree in Telecommunication from Warsaw University of Technology, Faculty of Electronics and Information Technology in 2013 and M. Sc. in 2014.



**Krzysztof PERLICKI**

Studies: Warsaw University of Technology, Department of Electronics and Information Technology, Warsaw, Poland; M. Sc. (1994), Ph.D. (1999), D.Sc.(2010)

Academic Positions: Professor at Institute of Telecommunications of

Electronics and Information Technology, Warsaw University of Technology, Poland  
 Scientific Activities: Fields of experience and research interests: high capacity optical transmission systems, optical access networks, attacks and security of physical layer in optical networks, test and measurement procedures for optical systems  
 Current activity: polarization effects in optical fiber, polarization multiplexing transmission systems, 80 scientific papers (english and polish), 4 scientific books (polish)  
 Membership: Optical Society of America, Federation of Telecommunications Engineers of the European Community



**Prof. Mirosław**

**SIERGIEJCZYK**, PhD. Eng.

- scientific fields of interest of the paper co-author concern among other issues of architecture and services provided by telecommunications networks and systems, especially from perspective of their

applications in transport, reliability and operation of telecommunications networks and systems, modelling, designing and organising telecommunications systems for transport.